Multi-scale AVA analysis

C.P.A. Wapenaar, Centre for Technical Geoscience, Laboratory of Seismics and Acoustics, Delft Univ. of Technology

Summary

Angle-dependent reflection functions are generally derived for step-functions of the medium parameters. However, outliers in well-logs, responsible for the main reflections, often behave quite different from step-functions. Unlike step-functions, these singularities are generally scale-variant. As a consequence, the AVA-behaviour of the reflection response of these singularities is scale-variant as well. In this paper we discuss a multi-scale AVA analysis procedure for the reflection response of scale-variant singularities. In particular we show that the proposed method yields information on the local singularity exponent α, which may prove to be a useful indicator in seismic characterization.

Introduction

Amplitude-versus-angle (AVA) analysis is generally based on a model consisting of two homogeneous layers, separated by a horizontal interface (see Castagna and Backus [1], Chapter I, for an extensive list of references). This implies that the medium parameters are assumed to behave as step-functions of the depth coordinate z, at least in a finite region around the interface. Since a step-function does not alter when its scale is changed, the AVA behaviour of the reflection response of a step-function interface is scale-invariant as well.

Looking at well-logs of, for example, the compressional wave velocity $c(z)$, it appears that the main outliers, responsible for the main reflections, often behave quite different from step-functions, see Figure 1. This motivates the investigation of the AVA behaviour of the reflection response of singularities other than the step-function. In this paper we will investigate the *multi-scale* AVA behaviour of scale-variant singularities.

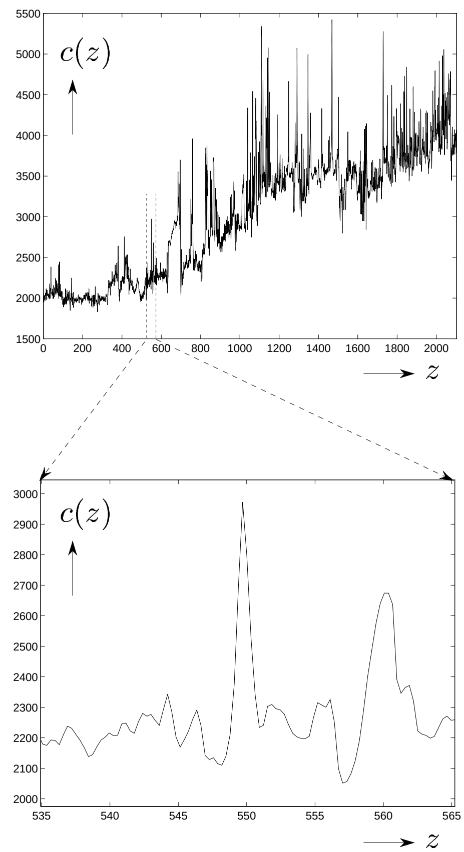

Fig. 1: *Well-log of P-wave velocity $c(z)$.*

A model for a scale-variant singularity

In this paper we consider singularities of the form

$$c(z) = \begin{cases} c_1|z/z_1|^\alpha & \text{for } z < 0 \\ c_2|z/z_2|^\alpha & \text{for } z > 0, \end{cases} \tag{1}$$

see Figure 2. Note that for $\alpha = 0$ this function reduces to the step-function. For $\alpha \neq 0$ this function nicely captures the singular behaviour of the type of outlier, observed in Figure 1 at $z = 550$ m. Moreover, the power spectrum of the derivative of $c(z)$ appears to be proportional to $|k_z|^{-2\alpha}$; Walden and Hosken [5] have observed a similar power-law behaviour for well-logs. Last, but not least, this singularity is *self-similar*, according to

$$c(\beta z) = \beta^\alpha c(z) \quad \text{for} \quad \beta > 0, \tag{2}$$

see Figure 2. This property will be exploited in the analysis of the multi-scale AVA behaviour of the reflection response of this singularity. Before we come to that, we first analyze the multi-scale behaviour of the singularity itself.

Multi-scale analysis of the singularity

The following analysis is due to Mallat and Hwang [4] and has been applied to well-logs by Herrmann [3]. Let the wavelet transform $\check{c}(\sigma, z)$ of $c(z)$ be defined as

$$\check{c}(\sigma, z) = \frac{1}{\sigma^\mu}\int_{-\infty}^{\infty} c(z')\psi\left(\frac{z'-z}{\sigma}\right)\mathrm{d}z', \quad (\sigma > 0), \tag{3}$$

with $\psi(z)$ being a proper analyzing wavelet, σ the scale parameter and μ a normalization coefficient that will be specified later. Replacing z' by $\sigma z'$, $\mathrm{d}z'$ by $\sigma \mathrm{d}z'$ and substituting equation (2) yields

$$\check{c}(\sigma, z) = \sigma^{\alpha+1-\mu}\int_{-\infty}^{\infty} c(z')\psi(z' - z/\sigma)\mathrm{d}z', \tag{4}$$

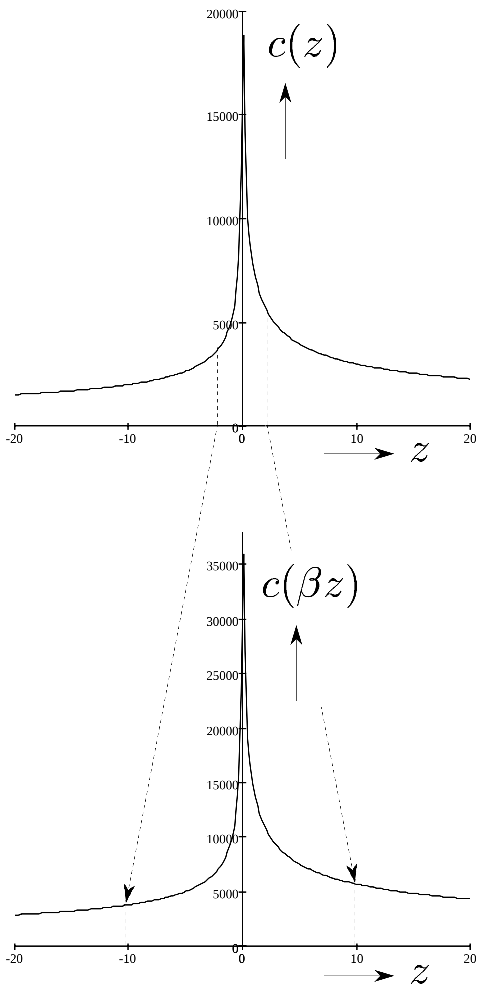

Fig. 2: *The self-similar singularity $c(z)$ of equation (1), with $\alpha = -0.4$, $c_1 = 2000$ m/s, $c_2 = 3000$ m/s, $z_1 = z_2 = 10$ m. The "zoom-factor" is chosen as $\beta = 0.2$, hence, the scaling factor β^α equals 1.904.*

or, comparing the right-hand side with that of equation (3),

$$\check{c}(\sigma, z) = \sigma^{\alpha+1-\mu}\check{c}(1, z/\sigma). \qquad (5)$$

Let $z = z_{\max}$ denote the z-value for which $|\check{c}(\sigma, z)|$ reaches its maximum for a fixed scale σ. Mallat and Hwang [4] define a *modulus maxima line* as the curve in the (σ, z)-plane that connects the local maxima $|\check{c}(\sigma, z_{\max})|$ for all σ. Choosing $\mu = 1$, it follows from equation (5) that the logarithm of the amplitude along the modulus maxima line is given by

$$\log|\check{c}(\sigma, z_{\max})| = \alpha \log\sigma + \log|\check{c}(1, z_{\max}/\sigma)|, \qquad (6)$$

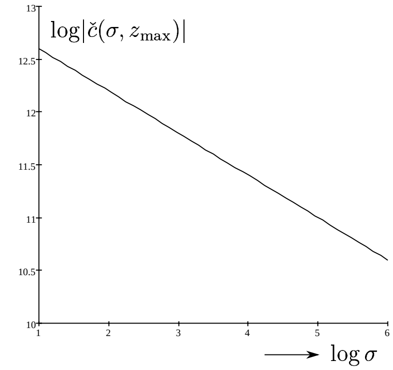

Fig. 3: *Amplitude along a modulus maxima line of $\check{c}(\sigma, z)$. The slope $\alpha = -0.4$ is equal to the singularity exponent of $c(z)$ in Figure 2.*

see Figure 3. It appears that the slope of this modulus maxima function is equal to the singularity exponent α. Herrmann [3] has applied this type of multi-scale analysis to well-logs. His results show that the modulus maxima functions of many singularities in well-logs exhibit a constant α behaviour (as in Figure 3) over a wide range of scales.

Multi-scale AVA analysis of the reflection response: numerical approach

Before we analytically derive the multi-scale AVA behaviour of the reflection response, we first discuss a numerical experiment and make some observations. For this experiment we consider a medium with its velocity defined by equation (1), with $\alpha = -0.4$, $c_1 = 2000$ m/s, $c_2 = 3000$ m/s and $z_1 = z_2 = 10$ m. We approximate this medium by a layered medium with homogeneous layers with a layer thickness of 1 m and we employ the standard 'reflectivity method' to model the plane-wave reflection and transmission responses. Figure 4 shows the incident and reflected waves in the (p, τ)-domain at 500 m above the singularity, Figure 5 the transmitted waves at 500 m below the singularity. For display purposes the impulse responses have been convolved with a Ricker wavelet with a central frequency of 32 Herz.

Let the wavelet transform of (p, τ)-data be defined as

$$\check{u}(p, \sigma, \tau) = \frac{1}{\sigma^\mu}\int_{-\infty}^{\infty} u(p, \tau')\psi\left(\frac{\tau' - \tau}{\sigma}\right)\mathrm{d}\tau'. \qquad (7)$$

The normalization coefficient μ will now be chosen such that for the special case of a step-function interface ($\alpha = 0$) the amplitudes of the transformed impulse response $\check{u}(p, \sigma, \tau)$ are scale-invariant. For this situation the reflection response is of the form $u(p, \tau) = r_0(p)\delta(\tau - \tau_0)$ and, consequently, $\check{u}(p, \sigma, \tau) = \sigma^{-\mu} r_0(p)\psi(\frac{\tau_0 - \tau}{\sigma})$. Hence, if we choose $\mu = 0$, the amplitudes in $\check{u}(p, \sigma, \tau)$ are scale-invariant for this situation.

We applied the transform defined in equation (7) (with $\mu = 0$)

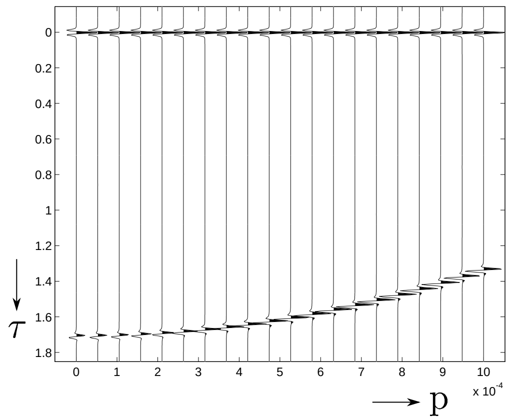

Fig. 4: Numerical reflection response, $\alpha = -0.4$.

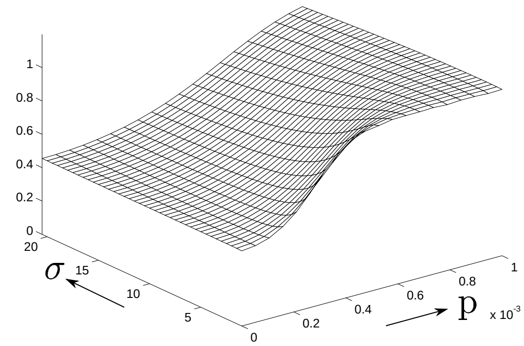

Fig. 6: Maximum amplitudes of the wavelet transform of the reflection response in Figure 4.

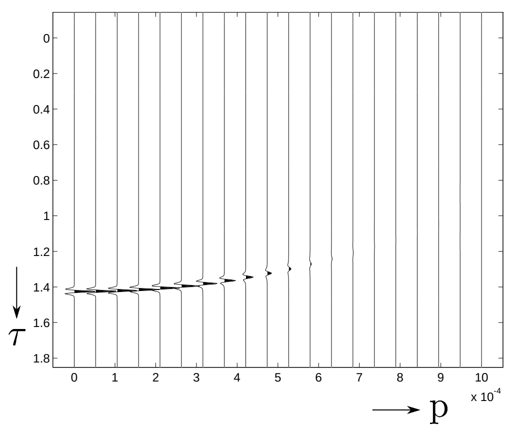

Fig. 5: Numerical transmission response, $\alpha = -0.4$.

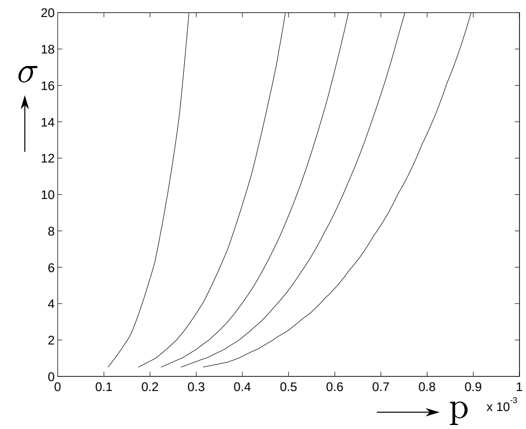

Fig. 7: Contours of constant amplitude in Figure 6.

to the reflection impulse response (Figure 4, without the Ricker wavelet). The maximum amplitudes of the modulus of each trace in $\check{u}(p, \sigma, \tau)$ are shown in the (p, σ)-plane in Figure 6. It is interesting to note that for $p = 0$ the amplitudes are scale-invariant (i.e., independent of σ), just as we derived above for the special case of a step-function interface. For $p \neq 0$, however, the amplitudes clearly show a scale-variant behaviour. This is also seen in Figure 7, which contains the contours of constant amplitude in Figure 6. Note that these contours would have been vertical lines if we had applied the same multi-scale analysis to the reflection response of a step-function interface.

Multi-scale AVA analysis of the reflection response: analytical approach

In this section we will explain the results observed in the previous section in an analytical way. At last year's SEG we showed already that the analytical normal incidence reflection and transmission coefficients are frequency-independent (Wapenaar [6]). This explains the scale-invariant amplitude behaviour for $p = 0$ in Figure 6. For oblique incidence we will not derive explicit expressions for the reflection coefficient, but we will derive its multi-scale AVA behaviour directly from the self-similarity relation (2). Our starting point is the wave equation in the (p, τ)-domain:

$$\left[\frac{\partial^2}{\partial z^2} - \left(\frac{1}{c^2(z)} - p^2\right)\frac{\partial^2}{\partial \tau^2}\right]u(z, p, \tau) = 0. \qquad (8)$$

Replacing z by βz, substituting equation (2) and multiplying the result by β^2 gives

$$\left[\frac{\partial^2}{\partial z^2} - \left(\frac{1}{c^2(z)} - (\beta^\alpha p)^2\right)\frac{\partial^2}{(\partial \beta^{\alpha-1}\tau)^2}\right]u(\beta z, p, \tau) = 0. \qquad (9)$$

The term between the square brackets is the same as in equation (8), with p replaced by $\beta^\alpha p$ and τ replaced by $\beta^{\alpha-1}\tau$. Hence, equation (9) is satisfied by $u(z, \beta^\alpha p, \beta^{\alpha-1}\tau)$ as well as

$u(\beta z, p, \tau)$. Consequently,

$$u(z, \beta^\alpha p, \beta^{\alpha-1}\tau) = f(\alpha)u(\beta z, p, \tau), \tag{10}$$

where $f(\alpha)$ is an undetermined α-dependent factor. In the upper half-space $z < 0$ we define an 'incident' wave field $u^{\rm inc}$ (with positive power flux) and a 'reflected' wave field $u^{\rm refl}$ (with negative power flux), both obeying equation (10) with one and the same factor $f(\alpha)$. For our analysis we do not need to specify this 'decomposition' any further. We relate these incident and reflected wave fields via a reflection kernel $r(p, \tau)$, according to

$$u^{\rm refl}(-\epsilon, p, \tau) = \int_{-\infty}^{\infty} r(p, \tau - \tau')u^{\rm inc}(-\epsilon, p, \tau'){\rm d}\tau', \tag{11}$$

with $\epsilon \to 0$. Replacing ϵ by $\beta\epsilon$, substituting equation (10) for $u^{\rm inc}$ and $u^{\rm refl}$ and comparing the result with equation (11) learns that the reflection kernel obeys the following similarity relation

$$r(p, \tau) = \beta^{\alpha-1} r(\beta^\alpha p, \beta^{\alpha-1}\tau). \tag{12}$$

Analogous to equation (7) (with $\mu = 0$), we introduce the wavelet transform of $r(p, \tau)$ by

$$\check{r}(p, \sigma, \tau) = \int_{-\infty}^{\infty} r(p, \tau')\psi\left(\frac{\tau' - \tau}{\sigma}\right){\rm d}\tau'. \tag{13}$$

Substituting equation (12), replacing τ' by $\beta^{1-\alpha}\tau'$ and ${\rm d}\tau'$ by $\beta^{1-\alpha}{\rm d}\tau'$ yields

$$\check{r}(p, \sigma, \tau) = \int_{-\infty}^{\infty} r(\beta^\alpha p, \tau')\psi\left(\frac{\tau' - \beta^{\alpha-1}\tau}{\beta^{\alpha-1}\sigma}\right){\rm d}\tau', \tag{14}$$

or, comparing the right-hand side with that of equation (13),

$$\check{r}(p, \sigma, \tau) = \check{r}(\beta^\alpha p, \beta^{\alpha-1}\sigma, \beta^{\alpha-1}\tau). \tag{15}$$

Let $\tau = \tau_{\rm max}$ denote the τ-value for which $|\check{r}(p, \sigma, \tau)|$ reaches its maximum for fixed p and σ. We define a *modulus maxima plane* as the plane in the (p, σ, τ)-space that connects the local maxima $|\check{r}(p, \sigma, \tau_{\rm max})|$ for all p and σ. It follows from equation (15) that the reflection amplitude in a modulus maxima plane behaves as

$$|\check{r}(p, \sigma, \tau_{\rm max})| = |\check{r}(\beta^\alpha p, \beta^{\alpha-1}\sigma, \beta^{\alpha-1}\tau_{\rm max})|. \tag{16}$$

The latter equation implies that contours of constant reflection amplitude in a modulus maxima plane are described by

$$p^{1-\alpha}\sigma^\alpha = {\rm constant}, \tag{17}$$

see Figure 8. Note that for $\alpha = -0.4$ these curves explain the numerically obtained contours in Figure 7. For $\alpha = 0$ these curves reduce to $p = {\rm constant}$, indicating again that the reflection response of a step-function interface is scale-invariant.

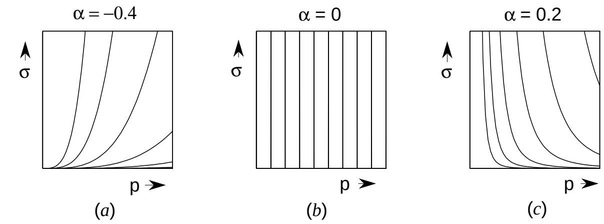

Fig. 8: *Curves of constant amplitude in the modulus maxima plane of the wavelet transformed reflection kernel* $\check{r}(p, \sigma, \tau)$*, for* $\alpha = -0.4$*,* 0 *and* 0.2*, respectively.*

Conclusion and discussion

The AVA-behaviour of the reflection response of a scale-variant singularity is scale-variant as well. It has been shown that the singularity exponent α governs the amplitude behaviour in the modulus maxima planes of the wavelet transformed reflection response (Figure 8). It is important to note that the analysis was based only on the similarity relation $c(\beta z) = \beta^\alpha c(z)$ (equation 2) rather than on the definition of the singularity (equation 1). This implies that the results (in particular equation 17) hold true for any singularity that approximately obeys the similarity relation (2) over a certain range of scales. In a companion paper (Goudswaard and Wapenaar [2]) we analyze the multi-scale AVA behaviour of the reflection response of real well-log singularities that approximately obey equation (2) in the *seismic* scale-range. It appears that the amplitudes in the modulus maxima planes approximately obey equation (17), which means that the singularity exponents α of these real well-log singularities can be resolved from the seismic data.

The exponent α may prove to be a useful indicator in seismic characterization, in addition to the other parameters that are commonly resolved by AVA inversion.

Acknowledgement

The author would like to thank the Dutch Technology Foundation (STW) for their financial support.

References

[1] J. P. Castagna and M. M. Backus. *Offset-dependent reflectivity – Theory and practice of AVO analysis*. Society of Exploration Geophysicists, 1993.

[2] J. C. M. Goudswaard and C. P. A. Wapenaar. Resolving well-log singularities from seismic data. In *Soc. Expl. Geophys., Expanded Abstracts*, 1997.

[3] F. J. Herrmann. *A scaling medium representation*. PhD thesis, Delft University of Technology, 1997.

[4] S. G. Mallat and W. L. Hwang. Singularity detection and processing with wavelets. *IEEE Trans. Inform. Theory*, 38(2):617–643, 1992.

[5] A. T. Walden and J. W. J. Hosken. An investigation of the spectral properties of primary reflection coefficients. *Geophys. Prosp.*, 33:400–435, 1985.

[6] C. P. A. Wapenaar. AVA for self-scaling interfaces. In *Soc. Expl. Geophys., Expanded Abstracts*, pages 1735–1738, 1996.